

Double differential cross sections of proton emission in neutron induced reaction on ^{27}Al

L. YETTOU^{1,a}, and M. BELGAID²

¹ Université Dr YAHIA Fares, Faculté des Sciences et de la Technologie Pôle universitaire 26000 Médéa, ALGERIA

² Laboratoire SNIRM, Faculté de Physique, USTHB BP 32 El Alia 16111 Bab Ezzouar, ALGERIA

Abstract. Double differential sections for proton emission on aluminium are presented for 40 MeV incident neutron energies. Angular distributions, energy differential and total production cross sections are obtained. The results are compared to existing data and to nuclear model calculations which include preequilibrium and compound decay mechanisms. The EMPIRE code treats these mechanisms in the framework of TUL model for multistep direct and NVWY model for multistep compound. The Hauser Feshbach theory is used to calculate emission from the compound nucleus, with a full conservation of spin and parity.

1 Introduction

Cross sections of many reactions, including preequilibrium reactions, play an important role for accelerator driven applications and for medical, shielding, and space applications at higher energies. In this work, some double differential cross sections for proton emission on aluminium based on nuclear model calculations with the EMPIRE reaction theory code [1] are calculated for 40 MeV incident neutron energies and compared with experimental data obtained from the EXFOR file (others data exist in the energy range from 28.5 to 62.7 MeV). In the EMPIRE code, the TRISTAN and ORION modules are based upon the Multi-step direct (MSD) quantum theory of pre-equilibrium processes formulated by Tamura, Udagawa, and Lenske (TUL) [2]. The ORION module calculates one and two-step cross sections with average state- independent form factors. These one and two-step cross sections are folded with the nuclear spectroscopic strength functions, derived in the TRISTAN module, which specify the microscopic nuclear structure properties within the framework of the Random Phase Approximation (RPA). The modelling of Multi-step Compound (MSC) processes follows the approach of Nishioka et al. [3]. Like most of the precompound models, the NVWY theory describes the equilibration of the composite nucleus as a series of transitions along the chain of classes of closed channels of increasing complexity. MSC calculations of the compound nucleus decay will be followed by the Hauser-Feshbach approach.

Full expositions of these models are given in Ref [1]. Here, we only give the key formulas that were used in this work.

^a e-mail : yettouleila@yahoo.fr

This is an Open Access article distributed under the terms of the Creative Commons Attribution-Noncommercial License 3.0, which permits unrestricted use, distribution, and reproduction in any noncommercial medium, provided the original work is properly cited.

2 Theoretical models

In the MSD theory the effective Hamiltonian in the open channel space is given as:

$$H = H^{opt} + H^{intr} + V^{res} \quad (2.1)$$

where H^{opt} describes the relative motion of projectile a and the target A , H^{intr} the intrinsic Hamiltonian of the asymptotically separated nuclei and V^{res} the residual effective projectile-target interaction.

The MSD approach treats the residual projectile-target perturbatively and the cross section is an incoherent super-position of n -step contributions as:

$$\frac{d^2\sigma}{d\Omega dE} = \sum_n \frac{d^2\sigma^{(n)}}{d\Omega dE} \quad (2.2)$$

where the multi-step cross sections are defined as:

$$\frac{d^2\sigma^{(n)}}{d\Omega dE} = \sum_{c=[nph]} P_c(E) |T_{c0}^{(n)}|^2 \quad (2.3)$$

which $P_c(E)$ defines the probability per energy to find the system in the configuration c and $|T_{c0}^{(n)}|^2$ defines the open channel T-matrix.

According the results given in Ref [1], the one-step cross section is expressed as:

$$\frac{d^2\sigma^{(1)}}{dE d\Omega} = \sum_{\lambda} S_{\lambda}(E) \overline{\frac{d\sigma^{(1)}}{d\Omega}}_{\lambda} \quad (2.4)$$

where $\overline{\sigma^{(1)}}$ is a reduced DWBA cross section and $S_{\lambda}(E)$ is the strength function.

According to Nishioka et al. [3], the average multistep compound (MSC) cross-section leading from the incident channel a to the exit channel b is given by:

$$\frac{d\sigma_{ab}}{dE} = (1 + \delta_{ab}) \sum_{n,m} T_n^a \Pi_{n,m} T_m^b \quad (2.5)$$

which summed all classes n and m . The transmission coefficients T_n^a describes the coupling between channel a and class n and $\Pi_{n,m}$ is the probability transport matrix. Pre-equilibrium compound proton emission was calculated in the Heidelberg multi-step compound (MSC) approach [4]. Equilibrium compound decay was treated within the Hauser-Feshbach statistical model [5] which calculations require transmission coefficients for particle emission, for energies spanning from zero to the maximum emission energy. The aluminium optical potential of A.Molina *et al.* [6], fitted to measured elastic scattering and total cross section data, was used for neutrons. For incident protons the optical potential of A.J.Koning *et al.* [7] was used. The optical potential of Bojowald *et al.* [8] was used for deuterons, and for tritons the Xiaohua *et al.* potential [9] was adopted. Finally, the potential of V.Avrigeanu *et al.* [10] was used for alpha and hellion particles. The level density for spherical nuclei was calculated in the framework of Gilbert et Cameron [11].

3 Results and discussions

Figures 1, 2 and 3 show calculated angular distributions for inclusive proton emission on aluminium for emission energies of 31.5, 37.5 and 41 MeV respectively. Theoretical prediction at 150°, 160° and 170° angles based on the quantum multistep TUL and NVWY theories are shown as continuous lines. The model largely overpredicts compound nucleus proton emission, and exhibit a good agreement for 37.5 and 41. MeV incident neutron energies.

In fact, the need for experimental data explains the failure of theory to understand these reactions. Also, the theoretical calculations agree at high angles ($> 90^\circ$), while the double-differential cross sections at small angles ($< 90^\circ$) underestimated (figures not shown in this paper). MSD mechanism is responsible for the major part of the cross section in this range. In fact, the compressional form factor should be used for the $l = 0$ transfer (default is the surface form factor). The different default is being used due to the numerical instabilities that happen occasionally when this physically-correct option is selected [1].

Figures 4, 5 and 6 show calculated energy differential cross sections and compared to existing data. The EMPIRE model calculations shown as the continuous lines in these figures account for the general features exhibited by experimental data, that is, the high-energy tail due to preequilibrium emission, the rise at low energies due to contributions from sequential compound nucleus decay, and the forward peaking of the data. However, an underprediction occurs above 30 MeV emission energies. Here the MSC mechanism plays an important role below 30 MeV emission energies and agrees poorly above this energy. While the MSD mechanism has a good predictive for the high emission energies.

Table I gives the experimental total cross sections [12] for proton production for 31.5, 37.5 and 41 MeV incident neutron energies compared to the theoretical values from model calculations (EMPIRE). The values agree poorly within the experimental errors.

Table 1. Total cross sections for proton production induced by 31.5, 37.5 and 41 MeV neutrons on aluminium (EMPIRE) are shown under the experimental data.

E_n (MeV)	Σ_{exp} (mb)	σ_{cal} (mb) (TUL +NVWY+HF models)
41.0	194±23	134.49
37.5	175±24	126.67
31.5	154±20	124.67

4 Conclusion

Our calculations using quantum-mechanical preequilibrium for proton production energy spectra $d^2\sigma/d\Omega dE$ for 40 MeV incident neutron energies with aluminium were compared to the experimental data 31.5, 37.5 and 41 MeV incident neutron energies. The calculations describe the experimental data well at high angles. While the energy differential cross sections and theoretical total cross sections are agree poorly with the experimental data. Complete double-differential and energy-differential cross sections have been calculated, but only some of them are presented here.

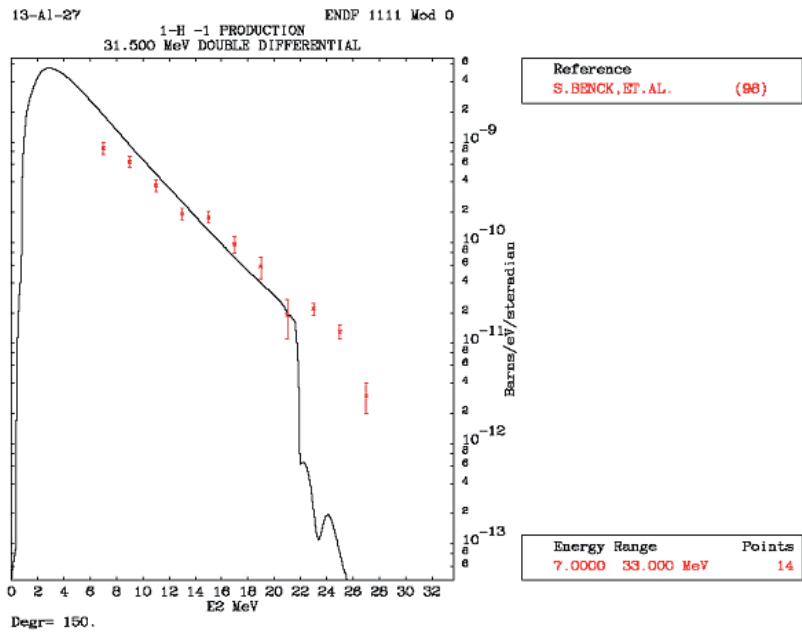


Fig. 1. Double-differential cross sections at 150° laboratory angles for the proton ejectile (red points). These points are obtained from the EXFOR data file for neutron-induced reactions on aluminium at 31.5 MeV. The continuous line is theoretical model prediction (EMPIRE) of the present work.

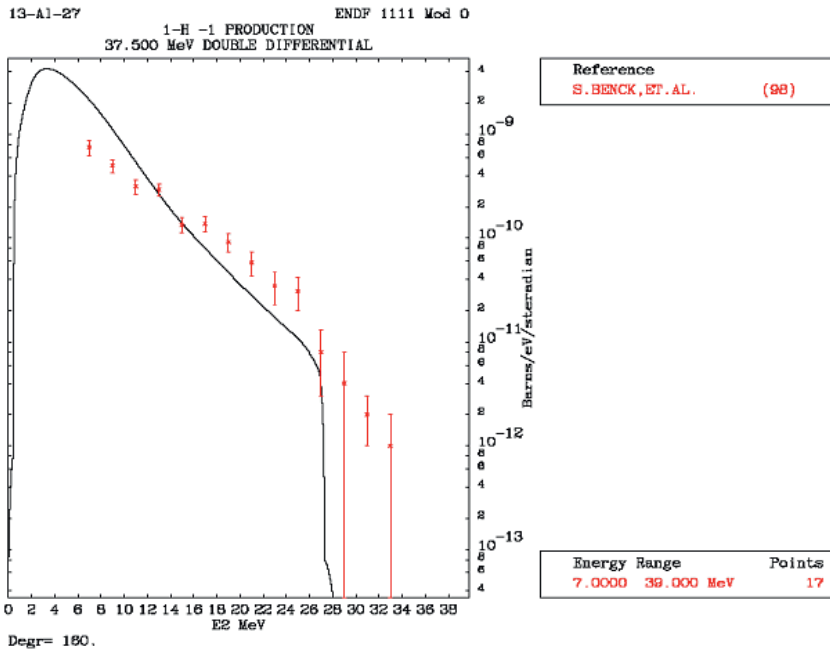


Fig. 2. Double-differential cross sections at 160° laboratory angles for the proton ejectile (red points). These points are obtained from the EXFOR data file for neutron-induced reactions on aluminium at 37.5 MeV. The continuous line is theoretical model prediction (EMPIRE) of the present work.

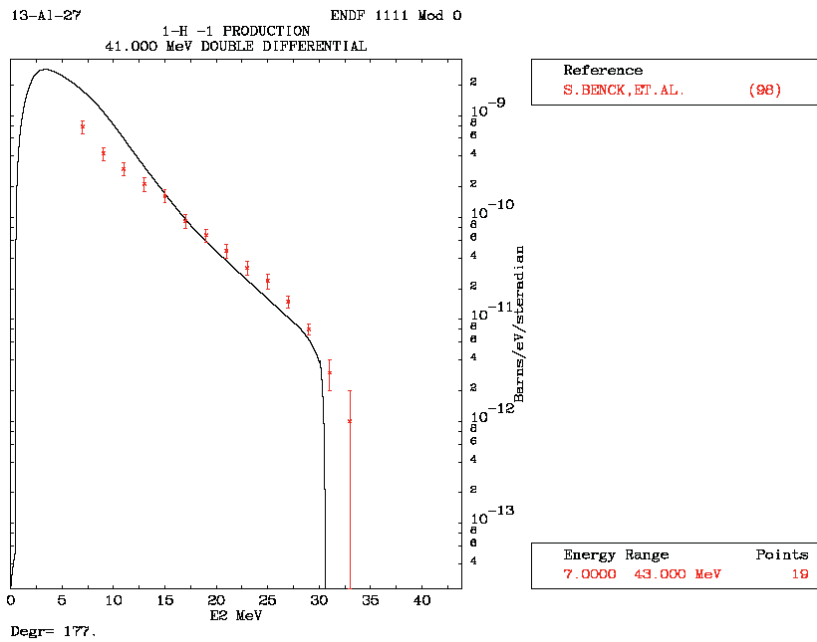


Fig. 3. Double-differential cross sections at 177° laboratory angles for the proton ejectile (red points). These points are obtained from the EXFOR data file for neutron-induced reactions on aluminium at 41 MeV. The continuous line is theoretical model prediction (EMPIRE) of the present work.

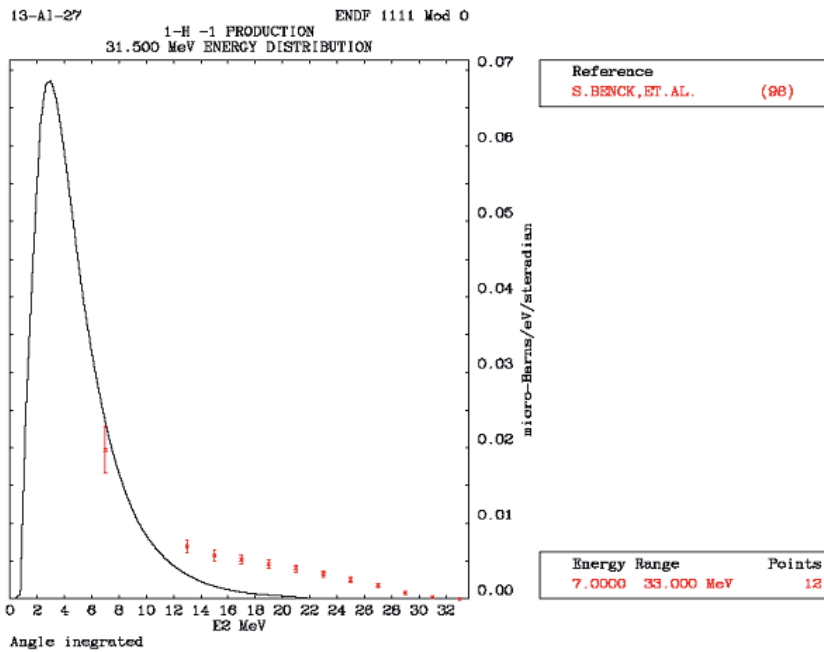


Fig. 4. $^{27}\text{Al}(\text{n}, \text{p})$ energy differential cross section for 31.5 MeV incident neutron energy. Continuous line shows theoretical calculations with TUL and NVWY models.

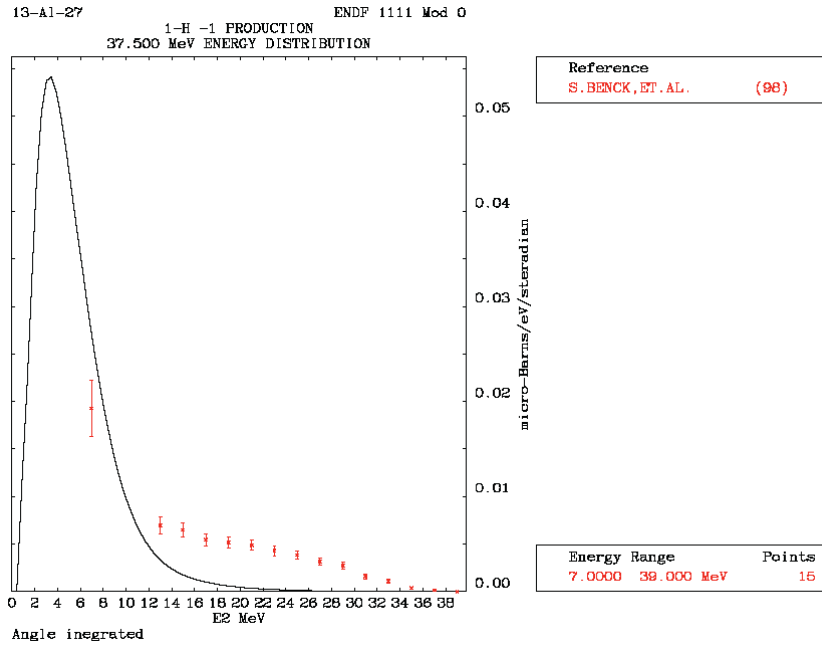


Fig. 5. ^{27}Al (n, p) energy differential cross section for 37.5 MeV incident neutron energy. Continuous line shows theoretical calculations with TUL and NVWY models.

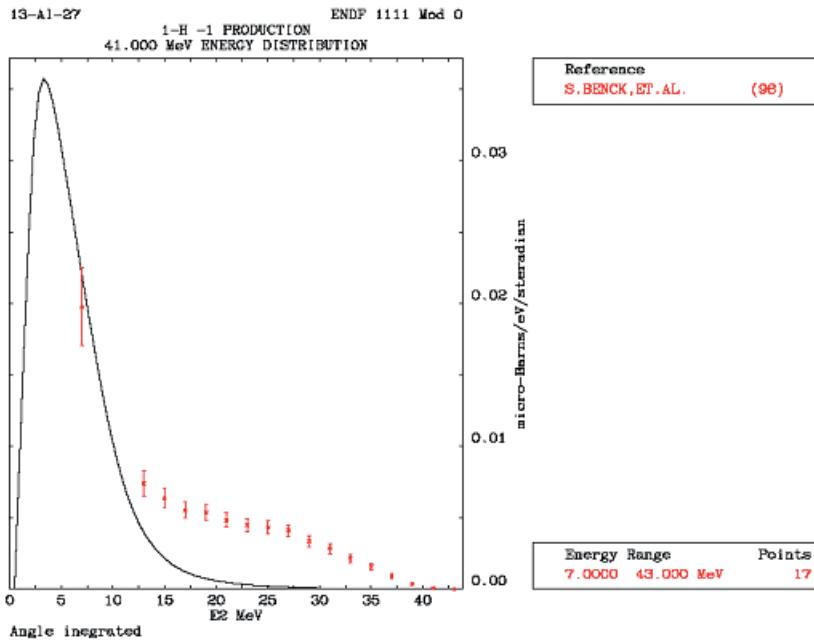


Fig. 6. ^{27}Al (n, p) energy differential cross section for 41 MeV incident neutron energy. Continuous line shows theoretical calculations with TUL and NVWY models.

References

1. M. Herman, P. Obložinsky, R. Capote et al., AIP Conf. Proc. **769** (2005), p. 1184. Code distributed online at <http://www.nndc.bnl.gov/empire2.19>.
2. T. Tamura, T. Udagawa, and H. Lenske, Phys. Rev. **C26**, 379 (1992).
3. H. Nishioka, J. J. M. Verbaarschot, H. A. Weidenmüller, and S. Yoshida. Ann. Phys. **172**, 67 (1986).
4. M. Herman, G. Reffo, and H. Weidenmüller, Nucl.Phys. **A553**, 124 (1992).
5. W. Hauser, H. Feshbach, Phys. Rev. **87**, 366 (1952).
6. A.Molina,R.Capote,J.M.Quesada,M.Lozano, Phys.Rev.**C65**, 34616 (2002).
7. A.J.Koning, J.P.Delaroche. Nucl. Phys. **A713**, 231 (2003).
8. J.Bojowald et al, Phys. Rev. **C 38**,1153(1988).
9. Xiaohua Li, Chuntian Liang, Chonghai Cai. Nucl.Phys.**A789**, 103-113(2007).
10. V.Avrigeanu, P.E.Hodgson, and M.Avrigeanu. Report OUNP-94-02 (1994) , Phys. Rev. **C49**, 2136 (1994).
11. A. Gilbert and A. G. W. Cameron, Can. J. Phys. **43**, 1446 (1965).
12. Mesures de Sections Efficaces Doublement Différentielles de Particules Chargées Légères Induites par Neutrons Rapides sur ^{16}O et ^{27}Al (En = 25 – 65 MeV) *Thèse de Doctorat en Sciences*, Université catholique de Louvain, Belgique.